Avoiding the Intercostal Arteries in Percutaneous Thoracic Interventions

Tihana Misura, MD, Dionysios Drakopoulos, MD, Milena Mitrakovic, MD, Tarja Loennfors, MD, Elias Primetis, MD, Hanno Hoppe, MD, Verena C. Obmann, MD, Adrian T. Huber, MD, PhD, Lukas Ebner, MD, and Andreas Christe, MD

ABSTRACT

The purpose of this study was to define relevant intercostal artery (ICA) anatomy potentially impacting the safety of thoracic percutaneous interventional procedures. An ICA abutting the upper rib and running in the subcostal groove was defined as the lowest risk zone for interventions requiring a supracostal needle puncture. A theoretical high-risk zone was defined by the ICA coursing in the lower half of the intercostal space (ICS), and a theoretical moderate-risk zone was defined by the ICA coursing below the subcostal groove but in the upper half of the ICS. Arterial phase computed tomography data from 250 patients were analyzed, revealing demographic variability, with high-risk zones extending more laterally with advancing age and with more cranial ribs. Overall, within the 97.5th percentile, an ICS puncture >7-cm lateral to the spinous process incurs moderate risk and >10-cm lateral incurs the lowest risk.

ABBREVIATIONS

ICA = intercostal artery, ICS = intercostal space, CT = computed tomography

The anatomical course of the intercostal arteries (ICAs) is of particular importance for the minimization of complications during percutaneous thoracic interventions. The reported rates of ICA laceration vary within the literature, but the overall incidence rate is <1% (1–5). However, inadvertent ICA laceration can result in clinically significant hemothorax and is associated with high rates of morbidity and mortality. The widely taught method for minimizing complications consists of inserting the needle or catheter "just above" the rib. Traditional anatomic teaching suggests that the ICA lies within the costal groove along the inferior border of the rib. However, many anatomic dissections using human cadavers have detected considerable variations in the positions of the neurovascular bundles, which may be located at a variable distance below the costal groove. The distance from the upper rib to the ICA in anatomic specimens has been proven to decrease as it courses anteriorly (6–13). Computed tomography (CT) angiography is a valuable tool for depicting vascular anatomy in a wide variety of anatomic regions (6,12).

The purpose of this study was to determine the distance from the spinous process in which the intercostal artery is located reliably in the upper half of the intercostal space (ICS) or in the subcostal groove, with a special focus on differences in anatomy between sexes and with advancing age.

MATERIALS AND METHODS

The study was conducted according to the guidelines of the Declaration of Helsinki and was approved by the institutional review board of the Cantonal Ethics Committee (Ethics Approval No. KEK 2020- 02281). All patients signed general consent forms for further use of their anonymized medical data.

Patient Selection

Patients who underwent arterial phase chest CT were included. Patients with CT data from the pulmonary arterial phase (pulmonary embolism protocol), CT data with inferior image quality due to motion artifacts or insufficient enhancement of the ICAs, and rib or chest wall pathologies were excluded. Group 1 (analyzed by radiologists T.M. and E.P.) consisted of 100 selected patients (10 consecutive patients per decade, starting from Jan 1, 2016), and Group 2 (analyzed by radiologists M.M. and T.L.) consisted of 150 selected patients (15 consecutive patients per decade, starting

Tables E1, E2 can be found by accessing the online version of this article on *www.jvir.org* and selecting the Supplemental Material tab.

J Vasc Interv Radiol 2022; 33:416–419
https://doi.org/10.1016/j.jvir.2021.12.026

from Jan 1, 2018). The data for the patients (from Jan 1, 2016 to Jan 1, 2021) were retrieved from the authors' radiologic information system (GE Healthcare, Chicago, Illinois). A total of 250 patients (25 patients per decade) were analyzed by the 2 radiologists in the group individually (not in consensus), with left- and right-sided measurements of 2 points of interest on 11 ICS levels, which resulted in 22,000 potential individual data points. After a break of 3 months, all original readers randomly re-measured 20 patients to assess the intraobserver agreement (880 measurements per reader).

Image Acquisition

CT angiography images were acquired by two 128-row CT scanners (Aquilion CXL; Toshiba, Tokyo, Japan and Somatom Definition Flash; Siemens Healthcare, Erlangen, Germany), with a slice thickness of 1 mm or less.

Image Analysis

Four radiologists (T.M., E.P., M.M., and T.L.) with 4, 20, 12, and 25 years of experience in chest imaging, respectively, performed the image analysis on a picture archiving and communication system (PACS) (Sectra; Linköping, Sweden). The ICAs originate from the aorta, pass around the vertebral bodies, and emerge into the ICS. At the beginning of their paravertebral intercostal course, they usually pass closer to the lower rib than the upper rib; with the "just above the rib" approach, 3 different theoretical risk zones of ICA injury were proposed: (*a*) high risk, ICA located in the lower half of the ICS, (*b*) moderate risk, ICA located in the upper half of the ICS, and (*c*) low risk, ICA located in the subcostal groove abutting the upper rib (Fig 1) (14).

The distances to these 2 transition points separating the 3 spaces were measured from the midline (spinous process) strictly horizontally on the coronal plane on both sides for each ICS level (Fig 2a–c). In cases where the artery was completely located in the upper ICS, the high-risk distance was measured from the midline (spinous process) to the most lateral edge of the vertebral body (earliest possible intervention side). For each ICS segment, the coronal plane was angulated continuously toward the thoracic spine using the maximum intensity projection with a slice thickness of 12 mm and an iteration of 1 mm. The ICA below the 12th rib was not assessed due to the lack of an ICS.

STUDY DETAILS

Study type: Retrospective, cross-sectional, observational study

Level of evidence: 4 (SIR-D)

Statistical Analysis

The Mann-Whitney U test for independent samples was used for comparing decades of life and ICS levels among men and women separately. The 97.5th percentile of the theoretical high- and moderate-risk distances were defined as the cutoff points for possible intervention sites. In addition, the maximum high- and moderate-risk distances of the study population were described (100th percentile). The inter- and intraobserver agreement was analyzed using the weighted kappa classification.

RESULTS

General Measurements

The median theoretical high- and moderate-risk distances for women were 2.9 cm (range, 1.0–9.3 cm) and 6.4 cm (range, 1.9–12.1 cm), respectively, from the spinous process to the lateral periphery. In men, the theoretical high- and moderate-risk distances were 3.3 cm (range, 1.0–9.7 cm)

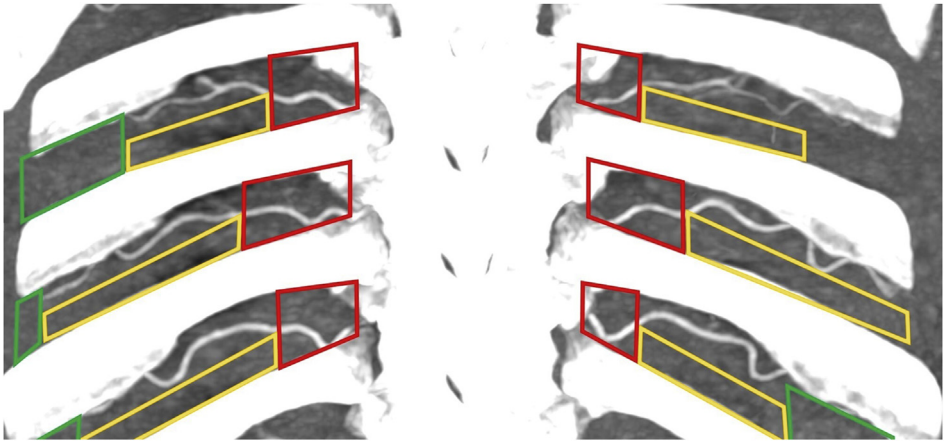

Figure 1. The paravertebral intercostal space was divided as follows: theoretical high-risk (red), theoretical moderate-risk (yellow), and low-risk zones (green) for punctures hugging the lower rib. To delineate these 3 zones, 2 transition points per side were identified: the point at which the artery crossed the halfway point of the intercostal space (where the artery started coursing closer to the upper rib than the lower rib), defining the transition from the theoretical high-risk zone to the theoretical moderate-risk zone (red to yellow), and the point at which the artery entered the costal groove, defining the transition from the theoretical moderate-risk zone to the theoretical low-risk zone (yellow to green).

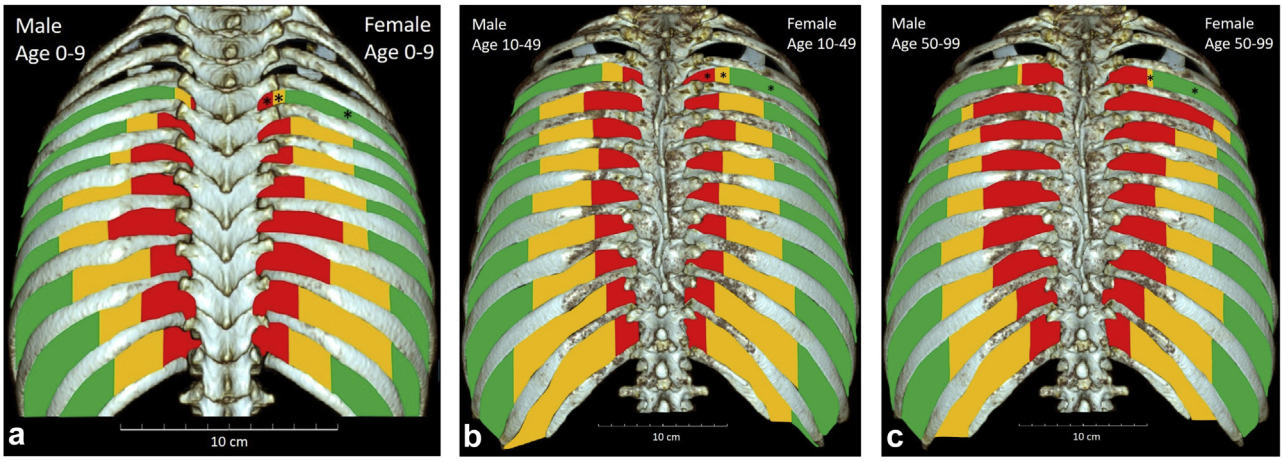

Figure 2. The theoretical high-risk, moderate-risk, and low-risk zones for thoracic interventions hugging the lower rib (red, yellow, and green, respectively), stratified by intercostal space level, sex, and age range. **(a)** 0–9 years, **(b)** 10–49 years, and **(c)** 50–99 years. Not enough intercostal arteries were visible in the third intercostal space in women for calculating the cutoff points; extrapolations are indicated with an asterisk.

and 6.9 cm (range, 1.2–14.0 cm), respectively (**Tables E1**, **E2**, available online on the article's Supplemental Material page at *www.jvir.org*). Using the 97.5th percentile, a puncture in women/men could be performed 5.1/6.5 cm away from the spinous process with theoretical moderate-risk, and a puncture could be performed with low-risk 10.0/10.4 cm lateral to the spinous process. Using the maximal range of measurements as the threshold, the high- and moderate-risk distances increased to 9.3/12.1 cm for women and 9.7/14 cm for men, respectively. In this study population, the ICA of the first and second ICS was practically invisible on arterial phase chest CT, and radiologists could not assess enough data for statistics.

Age-Dependent Space Measurements

The median theoretical high- and moderate-risk distances increased for women from 2.4 and 4.9 cm in the first decade to 3.6 and 6.6 cm in the 10th decade, respectively, with increments per decade of life (**Fig 3a**, **b**). The age-dependent and ICS level–dependent measurements for men and women are demonstrated in **Figure 2** and also listed in **Tables E1**, **E2** (available online at *www.jvir.org*).

Inter- and Intraobserver Agreement

The average interobserver agreement was moderate for the theoretical high- and moderate-risk distances, with a weighted kappa of 0.45 ± 0.19 and 0.43 ± 0.16, respectively. The average intraobserver agreement of the 4 readers was 0.56 ± 0.25 for the high-risk and 0.54 ± 0.24 for the moderate-risk distances.

DISCUSSION

The current work expands on that of Choi et al (6), Helm et al (12), and Yoneyama et al (13) by defining risk levels more conservatively, using the border where the ICA enters and stays in the upper half of the ICS as the delineation between theoretical high- and moderate-risk and the border where the ICA enters the costal groove as the delineation between the theoretical moderate-risk and the low-risk zones. The authors also stratified by sex and age and included more comprehensive measurements of all ICSs from T3 to T11, rather than single or limited levels. This study, involving 250 patients and using the 97.5th percentile of the theoretical high- and moderate-risk distances as the cutoff level, confirmed the variability of the arterial course with potentially extreme tortuosity posteriorly and proposes risk-stratified puncture zones.

Regardless of theoretical risk, interventional radiologists must occasionally choose a puncture site close to the midline due to a pathology being located close to the midline (eg, mediastinal abscess from esophageal leak, paravertebral lymph node, or medial lung biopsy). These punctures within the close proximity of the spinous process must be practiced with understanding of the risk and used only if clinically necessary. The identification of the ICA by duplex ultrasound before puncture can be helpful in these cases (15).

The classification into 3 ICS zones seems arbitrary, but was chosen to be a simple and practical system to reflect theoretical risk of introducing a puncture needle into the caudal half of the ICS. The observer agreement was only moderate, probably representing the difficulty of determining the point at which the ICS was halfway between ribs, which is why the study employed 2 readers for each patient to counteract subjectivity.

In conclusion, the variability of the ICA is age-dependent, and in the elderly, there is more tortuosity closer to the vertebral body, resulting in wider theoretical higher risk zones extending further laterally to the point where the ICA enters the costal groove. In fact, this juxtavertebral zone may be less risky for needle punctures in the upper half of the ICS compared with the lower half, and extends more laterally in men than in women. If clinically indicated to perform a puncture closer to midline, interventionalists should consider

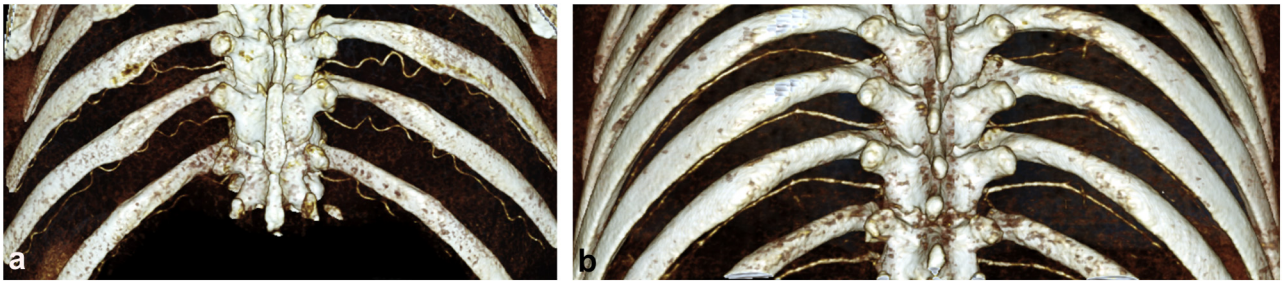

Figure 3. Age-dependent tortuosity of the paravertebral intercostal arteries depicted by surface reconstructions of computed tomography angiograms: **(a)** a 75-year-old patient demonstrated redundancy, tortuosity, and incursion into the lower half of the intercostal space more laterally, resulting in smaller zones of theoretical low-risk for intercostal puncture, compared with **(b)** a 35-year-old patient.

using ultrasound guidance to identify the ICA, or to puncture at least 7 cm lateral to the midline for a theoretically moderate-risk and at least 10 cm lateral to the midline for a theoretically lowest risk puncture.

ACKNOWLEDGMENTS

The authors thank the highly motivated team of medical technicians in their department for the excellent image acquisition.

AUTHOR INFORMATION

From the Department of Radiology (T.M., D.D., M.M., T.L., E.P., A.C.), Division City and County Hospitals, INSELGROUP, and Department of Diagnostic, Interventional, and Pediatric Radiology (V.C.O., A.T.H., L.E., A.C.), Inselspital, Bern University Hospital, University of Bern, Switzerland; and Department of Radiology (H.H.), Lindenhofspital Bern, Swiss Intervention Center for Microtherapy, Bern University, Bern, Switzerland. Received March 23, 2021; final revision received December 14, 2021; accepted December 16, 2021. Address correspondence to A.C., Department of Radiology, Division City and County Hospitals, INSELGROUP, Inselspital, Bern University Hospital, University of Bern, Tiefenaustrasse 112, CH-3004 Bern, Switzerland; E-mail: andreas.christe@insel.ch

T.M., D.D., L.E., and A.C. contributed equally to this work and are co-first authors.

None of the authors have identified a conflict of interest.

REFERENCES

1. Yamauchi H, Amemiya R, Shida D, et al. A case of spontaneous hemopneumothorax associated with uncontrolled massive bleeding after inserting thorathic drain. Kyobu Geka 1999; 52:965–968.
2. Muthuswamy P, Samuel J, Mizock B, Dunne P. Recurrent massive bleeding from an intercostal artery aneurysm through an empyema chest tube. Chest 1993; 104:637–639.
3. Carney M, Ravin CE. Intercostal artery laceration during thoracocentesis: increased risk in elderly patients. Chest 1979; 75:520–522.
4. Seneff MG, Corwin RW, Gold LH, Irwin RS. Complications associated with thoracocentesis. Chest 1986; 90:97–100.
5. Yacovone ML, Kartan R, Bautista M. Intercostal artery laceration following thoracentesis. Respir Care 2010; 55:1495–1498.
6. Choi S, Trieu J, Ridley L. Radiological review of intercostal artery: anatomical considerations when performing procedures via intercostal space. J Med Imaging Radiat Oncol 2010; 54:302–306.
7. Wraight WM, Tweedie DJ, Parkin IG. Neurovascular anatomy and variation in the fourth, fifth, and sixth intercostal spaces in the mid-axillary line: a cadaveric study in respect of chest drain insertion. Clin Anat 2005; 18:346–349.
8. da Rocha RP, Vengjer A, Blanco A, de Carvalho PT, Mongon MLD, Fernandes GJ. Size of the collateral intercostal artery in adults: anatomical considerations in relation to thoracocentesis and thoracoscopy. Surg Radiol Anat 2002; 24:23–26.
9. Muzrakchi AA, Szmigielski W, Omar AJ, Younes NM. Is the 10th and 11th intercostal space a safe approach for percutaneous nephrostomy and nephrolithotomy? Cardiovasc Intervent Radiol 2004; 27:503–506.
10. DeBiasi EM, Pisani MA, Murphy TE, et al. Mortality among patients with pleural effusion undergoing thoracentesis. Eur Respir J 2015; 46: 495–502.
11. Dewhurst C, O'Neill S, O'Regan K, Maher M. Demonstration of the course of the posterior intercostal artery on CT angiography: relevance to interventional radiology procedures in the chest. Diagn Interv Radiol 2012; 18:221–224.
12. Helm EJ, Rahman NM, Talakoub O, Fox DL, Gleeson FV. Course and variation of the intercostal artery by CT scan. Chest 2013; 143: 634–639.
13. Yoneyama H, Arahata M, Temaru R, Ishizaka S, Minami S. Evaluation of the risk of intercostal artery laceration during thoracentesis in elderly patients by using 3D-CT angiography. Intern Med 2010; 49: 289–292.
14. Netter FH. *Atlas of the human anatomy*. 7th ed. Philadelphia: Elsevier; 2018.
15. Kanai M, Sekiguchi H. Avoiding vessel laceration in thoracentesis: a role of vascular ultrasound with color Doppler. Chest 2015; 147:e5–e7.

Table E1. Age-Dependent Measurements of Theoretical High- and Moderate-Risk Zones (Distances From Spinous Processes in cm)

Age (y)	Women								Men							
	Theoretical high-risk zone								Theoretical moderate-risk zone							
	Median	Minimum	Maximum	2.5 percentile	97.5 percentile	Mean	SD	P*	Median	Minimum	Maximum	2.5 percentile	97.5 percentile	Mean	SD	P*
0–9	2.4	1.0	5.5	1.4	3.3	2.4	0.5 †		4.9	1.9	7.9	2.1	6.4	4.6	1.2 †	
10–19	2.7	1.5	6.0	1.7	4.1	2.7	0.7 ‡		6.3	2.4	10.7	2.7	9.6	5.8	1.9 §	
20–29	2.4	1.3	5.9	1.7	4.3	2.6	0.8 ‡		6.4	2.3	10.5	2.5	8.5	5.9	1.7 §	
30–39	2.6	1.3	5.8	1.5	4.3	2.8	0.8 §		6.2	2.0	9.9	2.6	8.7	5.9	1.7 ‡	
40–49	2.8	1.4	5.1	1.6	4.1	3.0	0.7 †		6.6	2.0	11.5	2.6	9.8	6.2	2.0 §	
50–59	3.2	1.9	5.3	1.9	4.7	3.2	0.8 §		6.6	2.1	11.0	3.2	8.9	6.6	1.6 §	
60–69	3.3	1.6	9.3	1.8	5.6	3.3	1.0 §		6.7	2.0	12.1	2.8	10.9	6.3	2.1 §	
70–79	3.2	1.9	7.6	2.0	6.0	3.3	1.0 †		6.8	2.5	12.0	2.8	9.9	6.2	2.1 †	
80–89	3.6	1.9	9.2	1.9	7.3	3.7	1.2 §		7.3	2.0	12.0	2.9	10.9	7.0	2.1 †	
90–99	3.6	1.9	7.0	2.1	5.4	3.6	0.9		6.6	2.3	11.8	3.3	10.1	6.4	1.7	
All ages	2.9	1.0	9.3	1.7	5.1	3.1	1.0		6.4	1.9	12.1	2.6	10.0	6.1	1.9	

Age (y)	Men															
	Theoretical high-risk zone								Theoretical moderate-risk zone							
	Median	Minimum	Maximum	2.5 percentile	97.5 percentile	Mean	SD	P*	Median	Minimum	Maximum	2.5 percentile	97.5 percentile	Mean	SD	P*
0–9	2.1	1.0	5.5	1.2	4.3	2.2	0.7 †		4.1	1.2	7.7	1.8	2.0	4.0	1.2 †	
10–19	2.9	1.6	6.5	1.9	5.3	3.1	0.9 §		6.5	2.3	11.9	2.7	9.2	6.1	2.0 §	
20–29	3.0	1.6	5.7	1.8	4.8	3.1	0.9 §		7.0	2.0	11.0	2.3	9.8	6.3	2.3 §	
30–39	3.0	1.5	6.8	1.7	5.6	3.3	1.1 §		7.0	2.2	13.0	2.8	10.2	6.5	2.2 §	
40–49	3.3	1.2	6.1	1.8	5.0	3.3	0.9 ‡		7.1	2.4	13.2	2.8	10.3	6.6	2.1 §	
50–59	3.4	1.8	9.7	2.0	7.4	3.7	1.3 ‡		7.1	2.4	12.4	2.7	10.2	6.7	2.1 §	
60–69	3.9	1.6	8.6	1.9	6.5	3.9	1.3 §		7.4	2.8	12.2	3.4	10.5	6.9	2.0 §	
70–79	4.0	1.8	9.4	2.0	7.2	4.1	1.4 §		7.8	2.5	14.0	2.9	12.2	7.1	2.6 §	
80–89	3.8	1.8	9.3	2.0	7.4	4.1	1.4 §		7.9	2.8	13.5	3.6	11.6	7.4	2.3 §	
90–99	4.0	1.4	8.4	2.2	7.2	4.1	1.3		7.7	2.6	11.2	2.8	9.8	7.3	1.9	
All ages	3.3	1.0	9.7	1.6	6.5	3.4	1.3		6.9	1.2	14.0	2.6	10.4	6.4	2.3	

*P value with respect to the next older decade.
†$P < .0001$.
‡$P < .05$.
§$P \geq .05$.

Table E2. ICS Level–Dependent Measurements of Theoretical High- and Moderate-Risk Zones (Distances From Spinous Processes in cm)

ICS	Women															Men													
	Theoretical high-risk zone								Theoretical moderate-risk zone								Theoretical high-risk zone								Theoretical moderate-risk zone							
	Median	Minimum	Maximum	2.5 percentile	97.5 percentile	Mean	SD	*P**	Median	Minimum	Maximum	2.5 percentile	97.5 percentile	Mean	SD	*P**	Median	Minimum	Maximum	2.5 percentile	97.5 percentile	Mean	SD	*P**	Median	Minimum	Maximum	2.5 percentile	97.5 percentile	Mean	SD	*P**
3	3.3	2.6	5.2	N/A	N/A	3.6	1.0	†	N/A	N/A	N/A	N/A	N/A	N/A	N/A	N/A	3.1	2.4	4.6	N/A	N/A	3.2	0.6	†	4.8	4.5	4.8	N/A	N/A	4.7	0.2	†
4	3.2	1.8	7.4	1.9	8.6	3.6	1.6	†	6.2	2.7	11.6	2.8	11.4	6.7	2.0	†	3.7	1.3	8.6	1.5	5.9	3.7	1.3	†	6.2	2.2	9.5	2.2	9.3	6.0	2.0	†
5	3.5	1.6	7.6	1.9	6.0	3.5	1.0	‡	6.1	2.0	11.8	2.9	9.5	6.2	1.7	†	3.8	1.1	9.2	1.6	7.3	3.9	1.5	†	6.7	1.5	12.4	2.6	9.8	6.3	2.2	†
6	3.2	1.0	8.4	1.6	5.5	3.2	1.0	†	6.3	1.9	12.0	2.5	9.4	5.9	1.9	†	3.7	1.2	9.3	1.7	7.0	3.8	1.4	†	6.9	1.5	12.8	2.6	10.0	6.4	2.2	†
7	3.2	1.3	7.9	1.6	4.9	3.2	0.9	§	6.5	2.0	12.0	2.6	9.2	6.1	1.9	†	3.5	1.1	9.7	1.6	7.2	3.7	1.4	†	7.2	1.7	13.0	2.7	10.2	6.6	2.3	†
8	3.3	1.4	9.2	1.9	5.5	3.3	1.0	‡	6.7	2.3	11.8	2.7	9.7	6.2	1.9	†	3.8	1.2	9.4	1.8	6.4	3.8	1.2	†	7.3	2.0	14.0	3.0	10.3	6.7	2.3	†
9	3.2	1.3	7.6	1.7	5.8	3.3	1.0	§	6.6	2.5	12.1	3.0	10.8	6.3	1.9	†	3.5	1.2	8.6	1.8	6.6	3.7	1.2	§	7.0	1.4	13.9	2.9	10.5	6.6	2.2	‡
10	2.7	1.3	6.4	1.8	4.3	2.8	0.7	§	6.5	2.1	12.0	2.8	10.0	6.1	1.9	‡	3.0	1.1	7.1	1.6	4.6	3.0	0.8	§	6.7	1.7	13.0	2.6	10.3	6.3	2.2	†
11	2.2	1.3	4.2	1.7	3.6	2.3	0.5		6.1	2.0	12.1	2.4	10.3	5.8	2.1		2.5	1.0	6.3	1.5	4.1	2.6	0.7		6.5	1.2	13.5	2.5	11.3	6.1	2.5	
All ICS	2.9	1.0	9.3	1.7	5.1	3.1	1.0		6.4	1.9	12.1	2.6	10.0	6.1	1.9		3.3	1.0	9.7	1.6	6.5	3.4	1.3		6.9	1.2	14.0	2.6	10.4	6.4	2.3	

ICS = intercostal space; N/A = not applicable.
**P* value with respect to the next older decade.
†$P \geq .05$.
‡$P < .05$.
§$P < .0001$.